

UNUSUAL PROPERTIES FOR THE NEA (436724) 2011 UW158

Bruce L. Gary
5320 E. Calle Manzana
Hereford, AZ 85615
BLGary@umich.edu

(Received: 2 October Revised: 21 November)

Near-Earth Asteroid 2011 UW158 was observed for 3.5 months with the Hereford Arizona Observatory 0.35-m telescope during the 2015 apparition. A phase curve slope of 0.023 ± 0.001 mag/deg was determined from r' -mag measurements for a phase angle range of 17 to 90 deg. This slope is used to estimate albedo = 0.39 ± 0.09 , $H = 19.93 \pm 0.11$, and diameter $D = 220 \pm 40$ m. The UW158 rotation period = 0.61072 h, which is greater than the “spin barrier” of the “rotation frequency vs. diameter” diagram, thus requiring internal cohesion.

Introduction

Near-Earth Asteroid (436724) 2011 UW158 has been referred to as the “platinum asteroid” because of widespread news coverage purporting that it was worth \$5.4 trillion for the platinum that it contained. Aside from this humorous story about its monetary value, UW158 turns out to have substantial scientific value because of its fast rotation in relation to its size.

The first observation of UW158, on 2015 Jun 17, was motivated by a listing of it as a target for JPL and Arecibo radar observations during its close approach in July. It was described as a candidate for a future human mission, based on a favorable orbit, and the radar web sites included a request for photometric observations prior to the scheduled radar observations. The specific need was for a rotation period for radar bandwidth planning purposes. The June 17 lightcurve showed that the rotation period was $\sim 1/2$ h. This was surprising since the H-G phase curve model used $H = 19.5$, based on 2011 discovery observations, and an asteroid this bright is usually larger than ~ 250 m. But it’s extremely rare for asteroids this large to rotate with a period < 2.2 hours. The two known exceptions are thought to be bodies having significant internal cohesion since a non-cohesive rubble pile of their size would “fly apart.” Smaller cohesion-less rubble pile asteroids can rotate faster without flying apart, but not larger ones.

The second observation, on Jun 20, confirmed the short rotation period (36.665 min). One key question became “Is the effective diameter really > 250 m?” To answer this question photometrically it would be necessary to verify that H wasn’t significantly fainter than 19.5 (e.g., $H > 20.5$), or that albedo wasn’t much greater than assumed (e.g., > 0.50), or some combination of these two assumptions. This goal was the motivation for creating a phase curve that could be used to evaluate both parameters.

The phase curve model of Belskaya and Shevchenko (2000), hereafter B&S, has been shown to be capable of doing this for large asteroids ($D > 10$ km) observed for phase angles (α) less than ~ 24 deg. Main-belt asteroids don’t have phase curve information beyond $\alpha \sim 24$ deg due to their orbit size, so it’s possible that the B&S relationship applies beyond this α limit. Indeed, the moon’s phase curve is linear (consistent with B&S) out to 45 deg (Gary, 2015d) and probably also out to 60 deg

(Hapke, 2015). If B&S is valid for these larger α , then it could be used for near-Earth asteroids (NEAs), whose viewing geometry is often limited to $\alpha > 24$ deg. With regard to asteroid size, there is no information showing that the B&S relationships can’t be used for smaller asteroids, but there is also no confirmation that it can be. If both supposed limitations of the B&S model could be overcome by showing that a small asteroid, observed at large α , conform to the B&S model, then it would become an important new tool for the photometric study of NEAs. Since radar observations of UW158 were planned, it was decided that this would be a good opportunity for evaluating the range of situations for which B&S can be used. In addition, UW158 showed promise as an asteroid that could be scientifically important because of its location in the “spin frequency/size” diagram.

Observations

A Meade 0.35-m fork-mounted Schmidt-Cassegrain telescope was used with a SBIG ST-10 XME CCD camera, binned 2x2. Hereford Arizona Observatory (MPC code G95) is located at 1420 m altitude in Hereford, AZ. Control of the telescope, dome, focuser, camera and offset autoguider was accomplished using *MaxIm DL* and 100-foot cabling in buried conduit. Image analysis was also performed using *MaxIm DL*. For each field-of-view, a median combine of all good-quality images was subtracted from individual images; these star-subtracted images were photometrically measured using an artificial star for reference. The images without star-subtraction were then photometrically measured, using the same artificial star for reference, but also including about two dozen stars designated as check stars. Both photometric CSV-files were imported into a spreadsheet; the star-subtracted mags for the moving asteroid were used with the non-star subtracted mags for the check stars, which served as candidate reference stars within the spreadsheet. This star-subtracting procedure has the advantage of greatly reducing the effect of background stars in the resulting lightcurve. Details of the observing, image analysis and spreadsheet procedures are given in Gary (2014, 2015a).

Unfiltered observations were calibrated using r' -mag’s of APASS stars (in the UCAC4 catalog). CCD transformation corrections were accomplished using a plot of reference star instrumental magnitude minus true (APASS) magnitude versus star color ($g'-r'$). This assured that each lightcurve segment was calibrated with an accuracy estimated to be < 0.010 mag. On one date, $g'r'i'z'$ filters were used to estimate the asteroid’s colors. On two dates, observations were made with $g'r'i'$ bands for the same purpose. On three dates, a SA-100 transmission grating was used to obtain spectra with $\sim 50:1$ resolution between 420 and 820 nm.

Sample Lightcurves

Figure 1 is a sample lightcurve showing a typical pair of different maxima per rotation.

Figure 2 is a phase-folded (rotation) lightcurve for the same data compared with data from four weeks earlier.

Notice in Fig. 2 that at rotation phase ~ 0.50 the r' -mag’s agree; the shape and brightness changes are limited to the other rotation phases. This is due to the maximum brightness during a rotation corresponding to one of the two broadside views (maximum solid angle), the lesser maximum corresponding to the opposite broadside view, while the minima are views closer to end-on. This illustrates the importance of choosing a rotation phase with maximum brightness for creating a phase curve.

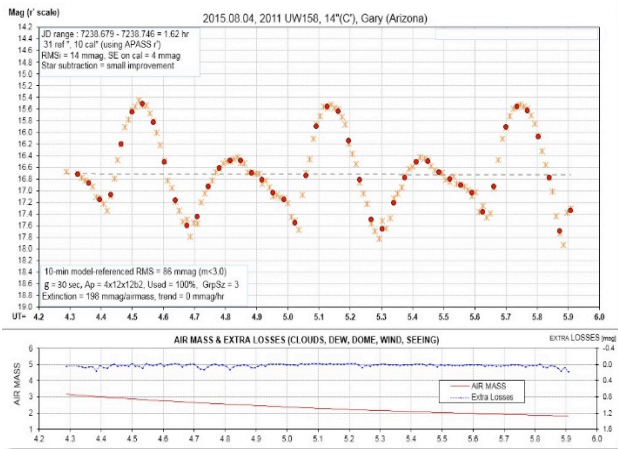


Figure 1. Lightcurve for Aug 4 (upper panel) showing 2.6 rotations. The lower panel shows air mass and un-modeled atmospheric losses due to clouds, dew, seeing, wind, etc.

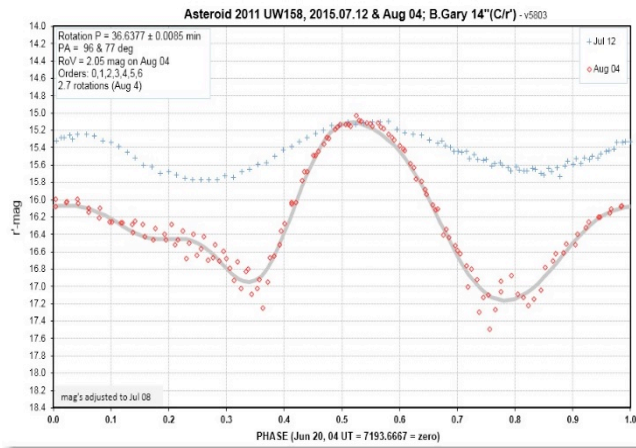


Figure 2. Phase-folded lightcurve for two dates showing change in amplitude and shape. The r'-mags have been adjusted to a standard date (Jul 8) using an H-G model with G = 0.15 to help in detecting which parts of the rotation have undergone change.

The entire set of rotation lightcurves show maxima at the same two rotation phases, as well as minima at similar rotation phases, and this shows that UW158 is not a tumbler.

Amplitude of Variation

It is evident in Fig. 2 that the rotation lightcurve amplitude (A), defined as peak-to-peak, varies greatly with date and that A can be large (2.05 mag). Figure 3 is a plot of A vs. date, with a smooth (high-order polynomial) fit.

The asteroid's closest approach to Earth occurred on Jul 20, when it was 6.4 times the moon's average distance. At this time it was moving fast along the 180 deg arc that is close to a great circle on the celestial sphere.

Whenever an asteroid moves through a 180 deg arc, there should be one location when it is viewed with an inclination (angle between line-of-sight and rotational axis) of 90 deg., *i.e.*, viewed within the asteroid's rotational equatorial plane. This will occur when A is maximum, provided shadowing is not important. A was maximum on Aug 4 (lightcurve shown in Fig. 2). It is likely that after Aug 4, with A decreasing monotonically, our view was of the asteroid's other hemisphere.

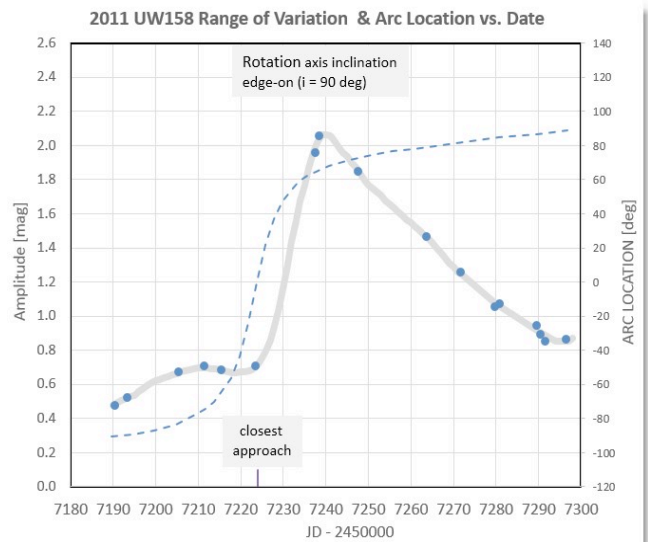


Figure 3. Rotation lightcurve amplitude (symbols) with a smooth fit, and location along the arc on the celestial sphere traversed during this 110-day interval (dashed trace).

Note that the Aug 4 value for $A = 2.05$ mag corresponds to a brightness ratio of 6.6:1. In other words, as the asteroid rotated (when our view was within the asteroid's equatorial plane), the solid angle could have varied by as much as 6.6 to 1. The association of brightness with solid angle assumes two things: 1) albedo is uniform across the surface, and 2) shadowing effects are small. Shadowing becomes important at large α , and α was 77 deg on Aug 4. If shadowing wasn't important on this date, then UW158 would be ~6.6 times longer than it is wide. But if shadowing was important for the end-on view (minimum brightness, rotation phases 0.34 and 0.78 in Fig. 2), then the ratio of dimensions would be smaller than 6.6:1.

Orientation of Rotational Axis

It is reasonable to begin with the assumption that UW158 resembles an ellipsoid, shown in Fig. 4, having radii a , b and c , where $c/b = 6.6$ (2.05 mag). An additional first assumption will be that dimensions "a" and "b" are the same.

A pole-on view will project the maximum solid angle for all rotation phases, given by $\pi \times b \times c / d$, where d = distance from Earth. An equatorial view will project a solid angle that ranges from $\pi \times a \times b / d$ to $\pi \times a \times c / d$. If $a = b$, we can convert rotation brightness ratio to inclination. The actual equation is quite complicated, so let's use a tube-model approximation for the ratio of maximum-to-minimum solid angle (brightness) as a function of inclination (i):

$$R(i) = x / (\sin i + x (\cos i)) \quad (1)$$

$$\text{where } x = c/b = c/a \text{ (i.e., } a = b) \quad (2)$$

For UW158, we know that $i = 90$ deg on about Aug 4, when $R(i) = 6.6$ (assuming uniform surface albedo and no shadowing effects). For example, the Jul 20 observation with $A = 0.70$, would then correspond to $i = 67$ deg. When each observation is converted to an i value, it is possible to draw arcs on the celestial sphere and their intersection will be one of the rotational axis pole positions. We don't yet know whether rotation is prograde or retrograde, so there will be two RA/DE pole locations. One pole position, according to this analysis, is at RA/DE = 17:30/+10. The



Figure 4. Ellipsoid with radii a , b , and c viewed with inclination ~ 45 deg (assuming rotational axis is parallel to “ a ”).

shortcoming of this method for deriving a rotational axis orientation is its shadowing assumptions. A better approach is to employ a shape-adjusting program designed specifically for fitting lightcurves made at specific viewing geometries; such an analysis is beyond the scope of this observational work.

Phase Curve: Albedo and Size

Creating a phase curve is most safely done for spherical asteroids, since their brightness won’t be affected by changes in solid angle as α varies. If UW158 had a circular cross-section orthogonal to the long axis (*i.e.*, $a = b$ in Fig. 4), then during each rotation there would be two equal brightness maxima corresponding to the same solid angle broadside view. The rotation lightcurve in Fig. 2 shows unequal maxima for Aug 4, thus revealing that the shape of UW158 is not the simple ellipsoid preferred for phase curve interpretation. The following phase curve analysis will be subject to this limitation.

UW158 was discovered on 2011 Oct 25 and must have been observed on several dates for determining an orbit. Apparently there were no lightcurve observations, so we don’t have A information or a rotation-maximum V-mag. If we assume that these astrometric observations were made at random rotation phases, we can use the adopted H-G model to estimate rotation-average V-mag for the α range of those observations (~ 14 – 21 deg). V-mag can be converted to r' -mag by subtracting 0.23 ± 0.08 (Gary, 2105e), based on the asteroid’s color as described below. It is assumed that rotation-maximum was between 0.1 and 0.6 mag brighter than rotation-average during the 2011 discovery observations.

Fig. 5 is a phase curve plot. The 2011 discovery r' -mags are plotted at their α range, with a rhombus-shaped symbol representing an estimate for rotation-maximum r' -mag. The 17 measurements for 2015 were made using the same observatory and the same analysis and calibration procedures, so they should share the same systematic calibration errors. The H-G model meant to represent rotation-maximum r' -mag (dashed trace) does not adequately fit all of the measurements. For $\alpha > 80$ deg, the measured r' -mag is brighter while for $\alpha < 50$ deg, the r' -mag is fainter. A greater G value would fit the data slightly better. However, there is greater interest in fitting the observations with a phase curve model that can be used to estimate geometric albedo and size.

B&S analyzed 33 well-studied main belt asteroids using a 3-term phase effect model first introduced by Shevchenko (1996, 1997):

$$V(\alpha) = V_0 + b \times \alpha - a/(1+\alpha) \quad (3)$$

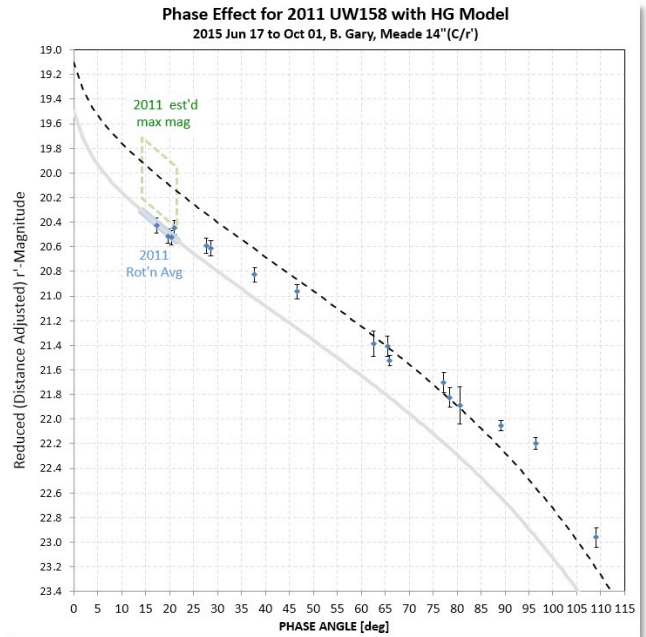


Figure 5. Rotation maximum r' magnitudes, adjusted to standard distance for 17 dates in 2015, with two H-G model fits: 1) $H = 19.5$, $G = 0.15$, and 2) $H = 19.1$, $G = 0.15$. The models are meant to fit rotation-average and rotation-maximum brightness, respectively. The symbols at $\alpha = 14$ – 21 deg are estimated r' -mag for the 2011 discovery observations.

where $V(\alpha)$ is V-mag at phase angle α , V_0 is V-mag at zero phase, “ b ” is phase coefficient (a slope term) fitted to $V(\alpha)$ measurements and “ a ” is an “opposition effect” (OE) amplitude term. B&S found that there was a strong correlation between the phase coefficient “ b ” and albedo, and also an inverted U-shape relationship between the OE amplitude term “ a ” and albedo. Their equation relating phase coefficient “ b ” and V-mag albedo at $\alpha = 0$, p_v , is:

$$b = 0.013(2) - 0.024(2) * \log(p_v) \quad (4)$$

where “ b ” has units of mag/deg and p_v is fractional geometric albedo. Hereafter, I will use the term “albedo” to be the same as p_v .

In Fig. 6, the observation date notations show that the first observation (Jun 17) was at $\alpha = 62$ deg, with α increasing to 109 deg (Jul 20), and then decreasing to 17 deg (Oct 01). It is noteworthy that on the occasions when measurements were made at the same α , but a month or more apart, there is r' -mag agreement.

The B&S model has a straight line slope parameter $b = 0.0228 \pm 0.0008$ mag/deg. Substituting this b value in the above equation (4) yields geometric albedo $p_v = 0.39 \pm 0.09$.

Since information for α close to zero is not present the size of OE isn’t measured. We shall use the B&S relation between OE and albedo. For an albedo of 0.39, they find that the OE term $a = 0.29 \pm 0.02$ mag. The solid trace in Fig. 6 includes the OE component.

Comparing Figures 5 and 6, the B&S model fits the measurements much better, with a good fit out to $\alpha = 96$ deg. The measurement at $\alpha = 109$ deg can be discounted as being affected by shadowing.

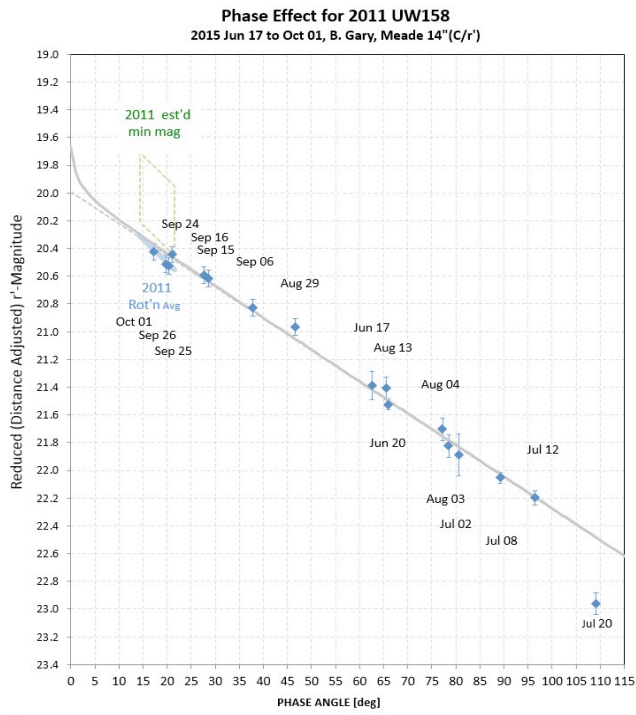


Figure 6. Same as Fig. 5, but with the B&S model fit. Observing date annotations are included.

The B&S model fit has $r' = 19.70 \pm 0.05$ at $\alpha = 0$. Converting to V-mag yields 19.93 ± 0.11 , which corresponds to H . Asteroid size can now be calculated using the standard equation:

$$D [\text{km}] = (1329 / \sqrt{\text{albedo}}) \times 10^{(-0.2 \times H)} \quad (3)$$

where albedo is a fraction. Setting $H = 19.93 \pm 0.11$, and albedo = 0.39 ± 0.09 , yields diameter = 220 ± 40 m. This is an equivalent diameter, corresponding to a circle with the same solid angle as that presented by a broadside view.

Whereas the B&S relationships were established for large asteroids with an $\alpha < 24$ deg, it is encouraging that the Fig. 6 phase curve for a smaller asteroid that was observed for $\alpha > 17$ deg exhibits such a good-quality fit using the B&S straight-line model. If a departure from a straight line model exists, it should manifest itself as a growing departure from linearity as α increases; there is no hint of this in the observations. Thus, one goal for the observations has been met: it is a “suggestive conclusion” of this work that the B&S phase curve model can be used for $\alpha \gg 24$ deg.

Claiming that the B&S relationships are valid for asteroids smaller than ~ 10 km is equivalent to claiming that the regolith covering of asteroids is similar for smaller asteroids. One approach for assessing the reasonableness of this hypothesis is to compare the size for UW158 obtained from radar observations with the size obtained photometrically using the B&S model.

Radar Size

JPL and the Arecibo Observatory observed UW158 using radar in mid-July, during closest approach. Fig. 7 is a frame from an Arecibo Observatory animation (P.A. Taylor, pers. comm.).

Arecibo Observatory radar images reveal an elongated shape that I estimate to be equivalent to an ellipsoid with 200 x 600 m outer

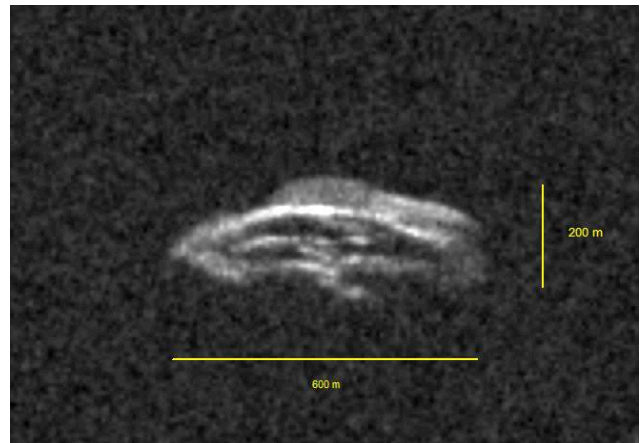


Figure 7. Arecibo Observatory radar image (one of a series of images from an animation showing rotation).

dimensions (Fig. 7). The rectangular equivalent dimensions appear to be 160 x 500 m. We should keep in mind that one of the radar dimensions (160 m) is “depth,” not a lateral dimension, so it is not directly related to solid angle. If we adopt 160 m for the missing (lateral) dimension, then we can calculate a size for deriving solid angle. The dimensions 160 x 500 m are equivalent to a circle with diameter 320 ± 50 m (where an arbitrary SE = 40 m per dimension is adopted). This equivalent diameter differs from the “photometric” diameter of 220 ± 40 m by an amount of 100 ± 65 m, which is not statistically significant. This can be viewed as supporting the argument that the B&S relationships can be used for small asteroids (and also determined by measurements at large α). This is a second “suggestive conclusion” of this work.

Rubble Pile vs. Solid Rock

Fig. 8 is in common use for characterizing the physical state of asteroids, based on their rotation spin-rate and size (estimated from H and albedo). Region A is where asteroids are small enough that inter-grain forces plus gravity are sufficient to hold the asteroid together for a wide range of spin frequencies. In other words, rubble piles as well as rocks may exist in Region A. Region B is where asteroids are rotating slowly enough ($P > 2.2$ h) that gravity is sufficient to hold rubble pile asteroids together; rock asteroids are also permitted. In Region C non-cohesive rubble piles are “forbidden” because they should fly apart (assuming plausible densities). In other words, only bodies where the constituents have significant cohesion, or are comprised of unfractured solid rock, should exist in Region C. The oft-cited 250 m size boundary was initially inspired by the pattern of avoidance in Region C, which was completely unpopulated until the discovery of 2001 OE84 by Pravec *et al.* (2002). Given that asteroid sizes are usually determined using estimated (or assumed) albedo, the locations of data points in this diagram should be viewed as horizontally oblong, causing the 250 m boundary to be better thought of as merely a most probable value within a range of sizes (as indicated using a shaded band in Fig. 8).

The radar dimensions (160 x 500 m, broadside view) are equivalent to a circular diameter of ~ 320 m (for broadside view), and a spherical equivalent volume with a diameter of ~ 290 m. According to the photometric solution, based on a phase curve with a B&S interpretation, all of the radar dimensions should be multiplied by $\sim 0.70 \pm 0.15$. Because of UW158’s elongated shape, the surface is located at distances from the rotation axis that can be as small as 100 m and as large as 600 m (represented by the

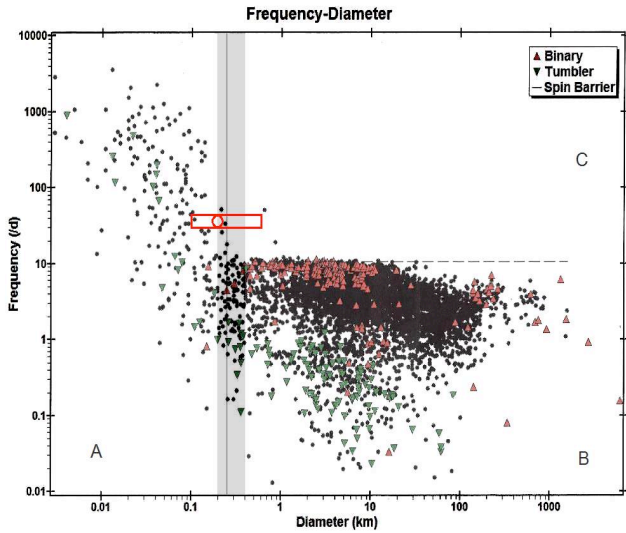


Figure 8. Plot of asteroid spin rate vs. diameter (based on Warner et al., 2009). The horizontal dashed line is the “spin barrier” and the vertical band defines a size boundary separating rubble piles permitted (to left) and cohesive or solid rock interiors only (to right) for spin rates above the spin barrier. A spherical version of UW158 is shown as a circle, within a rectangle representing a range of diameters corresponding to the smallest to the largest dimension for UW158.

rectangle in Fig. 8). The UW158 surface therefore straddles the 250 m “size barrier.” This means that we should consider the possibility that the ends of UW158 are experiencing a centrifugal force sufficient for loose regolith particles to “fly off,” leaving the ends bare rock, while the rest of the surface has the physical plausibility to retain regolith.

Visible Spectrum

UW158 was observed with g’r’i’z’ filters on Jul 2. The goal was to search for evidence of an I-band absorption feature at 0.92 microns. Details of these observations can be found at Gary (2015b). Fig. 9 shows the magnitudes at these four bands converted to flux, allowing for comparison with the sun’s flux spectrum. The asteroid’s spectral energy distribution (SED) is similar to the Sun’s except for a possible I-band absorption feature at 0.92 microns (due to olivine and pyroxene). The presence of

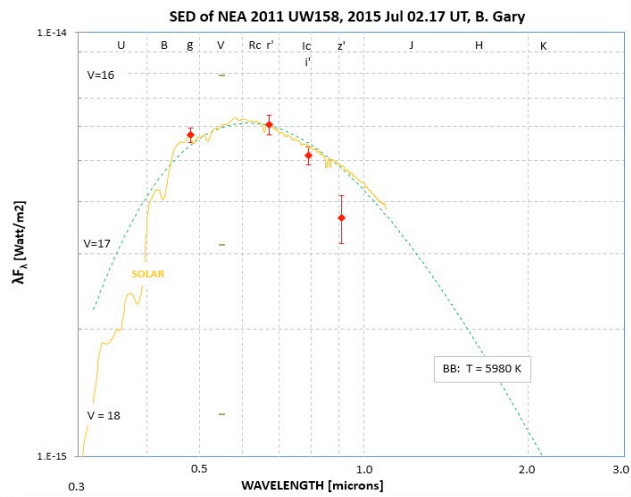


Figure 9. Jul 2 g’r’i’z’ magnitudes, converted to fluxes vs. wavelength (SED, spectral energy distribution), showing possible evidence for an I-band absorption feature at 0.92 microns.

such an absorption feature is not statistically significant but merely suggestive.

On Aug 13, g’r’i’ observations were also conducted. The average slope of “relative reflectivity” across this range of wavelengths was close to zero. This slope is uncertain due to the confounding effect of exposures with each filter not occurring simultaneously in the presence of fast changes of brightness.

On Jul 9 and 11, a SA-100 transmission grating was used to measure the UW158 visible spectrum with a spectral resolution of ~50. On each date, three solar-like stars were used for reference. The observing sequence, image processing and spreadsheet analysis are described in more detail at Gary (2015b,c). This spectrum is more uninfluenced by brightness variations due to rotation, since all wavelengths are measured simultaneously, so it should take preference over the spectrum based on g’r’i’ observations. The SA-100 spectrum shows a slightly red color, with B-V = +0.77 ± 0.10. Using this color allows the following conversion: V = r’ + 0.23 ± 0.08 (Gary, 2015e).

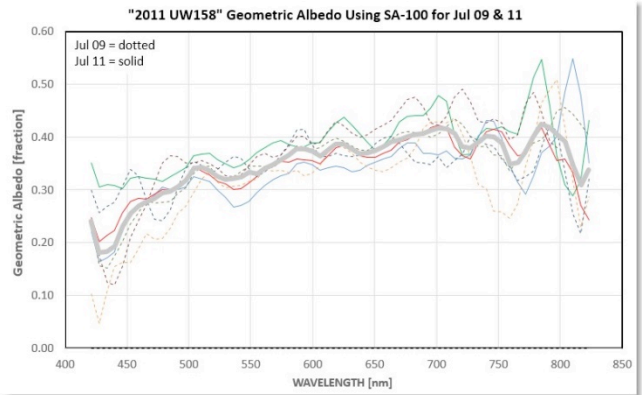


Figure 10. Transmission grating spectra of UW158 on two dates: Jul 9 and 11. The measurements are plotted as geometric albedo on the assumption of diameter being 220 meters.

A consensus albedo spectrum from the transmission grating observations on two dates is shown in Fig. 10, where geometric albedo is plotted for a 220 m diameter. Note that the geometric albedo at r’-band (~ 620 nm) is ~0.38 ± 0.03, in agreement with the phase curve analysis of 0.39 ± 0.09. The I-band absorption feature at 920 nm cannot be seen because sensitivity limited spectral coverage to < 820 nm.

Discussion and Conclusion

The 2011 UW158 phase curve, observed with a single telescope and reduction procedure, has been interpreted using the Belskaya and Shevchenko (2000) relationships to derive a geometric albedo of 0.39 ± 0.09 and an effective diameter of 220 ± 40 meters (for the rotation maximum brightness view). This albedo is confirmed using SA-100 transmission grating observations, calibrated using solar-like stars. The broadside dimensions are consistent with radar observations.

Since UW158 rotates with a period of 0.61072 h, it is “located” in a diagram of “spin rate vs. diameter” where rubble piles are permitted. This location in the spin/diameter diagram assumes a spherical diameter with volume equivalent to the estimated dimensions. However, UW158 is highly elongated, with a diameter ratio of at least 3.5 (based on both radar and photometry), so the ends of the asteroid are located far enough from the spin

axis that they are in a spin/diameter region where non-cohesive rubble piles are “forbidden.” Thus, while regolith particles may plausibly exist around the asteroid mid-section, the asteroid ends could be bare rock. Indeed, aside from a partial regolith coverage, UW158 must have a cohesive interior or be comprised by a solid rock; otherwise, the ends would fly away due to centrifugal force exceeding the gravitational one.

Future apparitions of UW158 won’t be as favorable as this one for another 93 years. Nevertheless, because of its uniqueness, even the less favorable apparitions at intervals of 2.056 years (*e.g.*, 2017 Sep with $V \sim 20.7$) will provide opportunities for additional observations with large telescope apertures for elucidating the nature of fast-spinning, rocky asteroids.

Acknowledgements

Asteroid ephemeris information was provided by Caltech’s Jet Propulsion Laboratory web site: <http://ssd.jpl.nasa.gov/horizons>. Calibration with SDSS magnitudes in the UCAC4 catalog was made possible through the use of the AAVSO Photometric All-Sky Survey (APASS), funded by the Robert Martin Ayers Sciences Fund. I want to record my appreciation to Dr. Arne Henden for initiating the APASS project; this is a sentiment I feel every morning after a night’s observations as I select APASS stars for calibration. Radar images were kindly provided by the Arecibo Observatory, which is operated by SRI International under a cooperative agreement with the National Science Foundation (AST-1100968), and in alliance with Ana G. Méndez-Universidad Metropolitana, and the Universities Space Research Association. The Arecibo planetary radar program is supported by the National Aeronautics and Space Administration under Grant Nos. NNX12AF24G and NNX13AQ46G issued through the Near-Earth Object Observations program. The “spin frequency/diameter” diagram (Fig. 8) is a modification of a graph at the IAU Minor Planet Center web site, which is based on data from the asteroid lightcurve database (Warner *et al.*, 2009).

References

- Belskaya, I.N., Shevchenko, V.B. (2000). “Opposition Effect of Asteroids.” *Icarus*, **147**, 94-105.
- Gary, B.L. (2014). *Exoplanet Observing for Amateurs*, Hereford, AZ: Reductionist Publications.
- Gary, B.L. (2015a). <http://brucegary.net/asteroids/>
- Gary, B.L. (2015b). <http://www.brucegary.net/UW158/>
- Gary, B.L. (2015c). <http://brucegary.net/SA/>
- Gary, B.L. (2015d). <http://www.brucegary.net/UW158/#Moon>
- Gary, B.L. (2015e). <http://www.brucegary.net/mags/#Examples>
- Hapke, B., Denevi, B., Sato, H., Braden, S., Robson, M. (2015). <http://onlinelibrary.wiley.com/doi/10.1029/2011JE003916/full>
- Pravec, P., Kusnirak, P., Sarounova, L., Harris, A.W., Binzel, R. P., Rivkin, A.S. (2002). “Large Coherent Asteroid 2001 OE84”, *Proc. Asteroids, Comets, Meteors (ACM 2002)*, Jul 29 – Aug 02, Tech. Univ. Berlin, Berlin, Germany (ESA SP-500).
- Shevchenko, V.G. (1996). “Analysis of the Asteroid Phase Dependencies of Brightness.” *Lunar Planet Sci.* **27**, 1193.
- Shevchenko, V.G. (1997). “Analysis of Asteroid Brightness-Phase Relations.” *Solar System Res.* **31**, 219-234.
- Warner, B.D., Harris, A.W., Pravec, P. (2009). “The Asteroid Lightcurve Database.” *Icarus* **202**, 134-146. Updated 2015 Sept. <http://www.minorplanet.info/lightcurvedatabase.html>